A Novel AM Modulation Technique for Solid-State Transformers with Reduced Conversion Stages and Enhanced Efficiency

Hesamodin Abdoli[1], Ghasem Rezazadeh[2,*], Javad Shokrollahi Moghani[3], And Sadegh Vaez-Zadeh[4]

[1] *Department of Electrical Engineering, Amir Kabir University of Technology (Tehran Polytechnic), Tehran, Iran. E-mail: hesamodinabdoli@gmail.com , Phone: +989128931048*

[2] *School of Electrical and Computer Engineering, College of Engineering, University of Tehran, Tehran, Iran. E-mail: G.rezazadeh@ut.ac.ir , Phone: +982182084217*

[3] *Department of Electrical Engineering, Amir Kabir University of Technology (Tehran Polytechnic), Tehran, Iran. E-mail: moghani@aut.ac.ir , Phone: +982164543349*

[4] *School of Electrical and Computer Engineering, College of Engineering, University of Tehran, Tehran, Iran. E-mail: Vaezs@ut.ac.ir , Phone: +982161114916*

**Corresponding author: Ghasem Rezazadeh (g.rezazadeh@ut.ac.ir).*

***Abstract*— Recent advancements in smart grid technology and the increasing adoption of renewable energy sources highlight the need for an alternative to conventional transformers. Traditional transformers suffer from issues such as lack of controllability, large size, and weight, making them less suitable for modern grid applications. Solid-State Transformers (SSTs) have emerged as an attractive solution due to their controllability, compact size, and power density. In this paper, a novel SST structure is proposed with a new modulation technique, which reduces one of the baseline energy conversion stages by directly converting DC voltage into a medium-frequency waveform with a controlled amplitude. The proposed structure simplifies the control system and enhances power density compared to traditional SSTs. The effectiveness of the proposed structure is validated through both simulation and experimental results, which demonstrate improved performance in terms of efficiency, harmonic reduction, and reduced system cost.**

***Index Terms*— Cascaded H-Bridge, Multilevel converter, PV application, Solid-State Transformer (SST).**

I. INTRODUCTION

Some promising research has been done Solid-State Transformers (SSTs) have gained significant attention due to their superior power density compared to traditional transformers, making them highly suitable for applications with stringent volume and weight constraints, such as traction systems and electric vehicles [1], [2]. One of the key advantages of SSTs is their ability to precisely control active power, reactive power, voltage, and current, which allows for better regulation and flexibility in power distribution [3]. This capability simplifies operations such as increasing output current, decoupling the output frequency from the input, and achieving a power factor of one, all of which are complex tasks for conventional transformers [3]-[6].

SSTs are increasingly deployed in a wide variety of applications, including smart grids, photovoltaic (PV) systems [7], [8], wind energy systems [9]-[11], and other renewable energy systems that are integral to modern power distribution and management strategies [5], [6], [12] (as shown in Fig. 1). Recent advancements in high-frequency transformer design have further improved the efficiency and reliability of SSTs, making them more viable for medium- and high-power applications [23], [24]. Moreover, hybrid converter-based SSTs have been proposed to enhance power conversion efficiency while reducing switching losses [25], [26].

In applications where high voltage and power are required, multilevel converters or matrix structures are commonly used in SSTs to 1) reduce THD in the output voltage, 2) minimize stress on the power switches, and 3) enhance the overall efficiency and reliability of the system [13], [14]. Recent studies on modular multilevel converter (MMC)-based

SSTs indicate that MMC structures improve voltage balancing and provide better scalability for high-power applications [27], [28]. Additionally, modularized diode rectifiers have been explored as an alternative topology to improve SST performance and efficiency [29].

A baseline SST configuration designed to inject PV electrical power into the grid typically involves several stages of conversion (as shown in Fig. 2). First, a DC voltage is converted into AC voltage at the grid frequency through an inverter. Then, a primary AC-AC converter on the transformer's primary side further converts the low-frequency AC voltage into a medium-frequency voltage with a sinusoidal envelope. This medium-frequency voltage is then adjusted at the secondary side of the transformer using a secondary AC-AC converter [15], [16]. However, new topologies based on hybrid switched-capacitor LLC-SRC converters have been introduced to improve voltage regulation and minimize the number of power conversion stages [30].

Although the baseline SST configuration is widely used, it suffers from a few critical drawbacks. The system requires multiple stages of energy conversion, involves extensive deployment of power electronics components, and demands complex control systems, which significantly increase both initial costs and maintenance requirements [17], [18]. These challenges highlight the need for an innovative SST design that minimizes the number of energy conversion stages while maintaining performance and reducing overall system costs [19], [20]. Reliability and redundancy considerations in modular SST designs have also been investigated to ensure long-term stability and reduce failure rates [31].

Solid-State Transformers (SSTs) can be categorized based on their power and voltage levels, as different applications require specific topologies optimized for their operating conditions. At low-voltage levels, SSTs are primarily designed for residential and commercial applications, where power ratings typically range from several kW to a few hundred kW. These systems often utilize single-stage AC-AC or dual-stage AC-DC-AC converters to achieve compact designs with high efficiency [26], [30].

For medium-voltage applications, SSTs are widely employed in distribution networks and industrial systems, requiring power levels from hundreds of kW up to several MW. Common topologies include modular multilevel converters (MMC) and hybrid switched-capacitor converters, which enhance power scalability and reduce stress on semiconductor devices [25], [27]. Some of these configurations incorporate back-to-back resonant converters to improve soft-switching operation and enhance overall system performance [34], [35].

At high-voltage levels, SSTs are integrated into power transmission systems and high-power industrial applications, where voltages exceed tens of kV and power ratings surpass tens of MW. These SSTs often rely on multiport high-frequency transformers combined with advanced power conversion architectures, such as four-port SST designs and medium-voltage MMC-based structures to ensure stable and efficient energy conversion [31], [32].

This classification provides a clearer understanding of how SST architectures evolve with increasing power and voltage demands, laying the foundation for the specific power level and topology analyzed in this study.

In this paper, we propose a novel modulation technique tailored for multilevel inverters, designed to generate a variable-amplitude multilevel AC voltage waveform. By employing this technique, we combine two conventional energy conversion steps into one, as illustrated in Fig. 3. Specifically, the modulation is applied as a grid frequency envelope control method, directly converting the DC voltage into a medium-frequency AC waveform. The medium-frequency harmonics present in the output voltage of the Multilevel Inverter (MLI) are then eliminated by the secondary converter at the transformer's output [21], [22]. This method aligns with recent advancements in high-power SSTs designed for medium-voltage distribution grids [32], [33], [34]. This simplified and integrated approach makes the proposed SST particularly advantageous for PV applications.

The paper is structured as follows: Section II provides a detailed explanation of the baseline SST structure. Section III discusses the fundamentals of the Amplitude Modulation (AM) technique used in the proposed SST. In Section IV, simulation results from the SIMULINK/MATLAB environment are presented to validate the performance of the proposed structure. Finally, Section V presents the experimental results of a prototype converter, which are used to assess the analytical and simulation results.

II. BASELINE SST STRUCTURE AND ITS OPERATION STAGES

The baseline SST design, as shown in Fig. 2, is responsible for converting direct current DC voltage into AC voltage at the grid frequency [1]. This configuration typically involves three distinct power electronic stages: an inverter and two AC-AC converters, with a medium-frequency transformer used. Each of these stages plays a critical role in ensuring the efficient operation of the SST, especially in applications such as renewable energy integration and electric grid power distribution. This multi-stage conversion process, though effective, introduces several challenges related to efficiency, cost, and complexity, which motivates the search for alternative, more simplified designs in modern SST implementations. Below, we describe the key stages in the operation of a baseline SST design.

A. STAGE ONE:

In the first stage, depicted in Fig. 2, the multi-level inverter is responsible for converting the input DC voltage into a multi-level AC voltage with the grid frequency. In baseline SSTs, the multi-level inverter structure is often based on the Cascaded H-Bridge (CHB) topology, which is particularly beneficial in applications where multiple independent DC power sources are available. This feature is especially advantageous in scenarios like the integration of solar power into the grid, where each panel or string of panels can be connected to a separate DC input. The CHB inverter exhibits favorable characteristics for such applications because it allows for modularity and scalability, and it helps to reduce THD of the output AC waveform.

In this configuration, the inverter operates with various modulation techniques, such as phase-shifted or level-shifted modulation, to control the output voltage and minimize the harmonic content in the output signal. The modulation index, denoted as A plays a crucial role in determining the output waveform's amplitude. The reference waveform for the inverter is given by the following equation:

$$F_1(t) = Asin(\omega_1 t) \quad (1)$$

where ω_1 represents the grid frequency, and A is the modulation index that defines the amplitude of the sinusoidal waveform. This waveform forms the first stage of the SST and provides the AC signal that will be further processed in the subsequent stages.

B. STAGE TWO:

In the second stage of the SST, a Pulse Width Modulated (PWM) AC-AC converter is used to transform the low-frequency AC output from the inverter into a medium-frequency AC waveform. The AC-AC converter modulates the sinusoidal waveform generated in the previous stage, adjusting its frequency to ω_2. The medium-frequency waveform is crucial because it serves as the input to the medium-frequency transformer in the next stage, which increases the voltage to the required level for grid injection.

The waveform generated by the AC-AC converter in this stage is described by the following equation:

$$F_2(t) = (-1)^{[\omega_2 t]} \quad (2)$$

The working frequency ω_2 is associated with the medium-frequency transformer's operational frequency. This stage of conversion ensures that the medium-frequency waveform is generated, which is essential for stepping up the voltage in the following transformer stage. The reference waveform of the primary AC-AC converter is illustrated in Fig. 2, demonstrating how the output from the first stage is modulated in frequency by the AC-AC converter

C. STAGE THREE:

The third stage of the SST involves another AC-AC converter, a dual-sided H-Bridge converter that operates at three levels. This converter is responsible for transforming the medium-frequency AC signal produced in the previous stage into a multi-level AC voltage at the grid frequency. The H-Bridge converter utilizes a zero-crossing detection circuit that senses the moment when the voltage crosses zero, alternating with the frequency ω_2. This detection process allows for the elimination of medium-frequency harmonics, ensuring that the output waveform consists primarily of the fundamental grid frequency harmonic.

The working frequency ω_2 is used in both the primary and secondary AC-AC converters, meaning that both converters operate at the same frequency. The transformation function of the H-Bridge converter closely resembles that of the primary side AC-AC converter, and its logic can be expressed as follows:

$$F_3(t) = (-1)^{[\omega_2 t]} \quad (3)$$

This transformation process essentially filters out the medium-frequency harmonics, leaving behind a clean waveform at the grid frequency. This is crucial for ensuring that the final output meets the grid requirements and is compatible with existing power distribution infrastructure

The total transformation function of the baseline SST, which represents the combined effect of all three stages, is given by:

$$F(t) = N \times F_1(t) \times F_2(t) \times F_3(t) = NAsin(\omega_1 t) \quad (4)$$

Where N is the turns ratio of the transformer. As seen from this equation, the primary frequency from the inverter ω_1 is the dominant frequency in the final output waveform, with the medium-frequency harmonics effectively eliminated. The inverter, therefore, plays the key role in controlling the output frequency and voltage, ensuring that the SST operates in a stable manner and maintains the desired output characteristics.

The inverter also serves as the central component in the closed-loop control system of the SST, where it continuously adjusts its operation to maintain optimal performance in terms of voltage regulation, harmonic reduction, and efficiency. This control system is essential for ensuring that the SST can operate reliably over a range of varying input conditions, such as changes in solar generation or grid demand.

In this expanded description of the baseline SST design, the multi-stage process of converting DC to AC and stepping up voltage to grid levels has been explored in greater detail. Each stage—DC to multi-level AC conversion,

low-frequency AC to medium-frequency AC conversion, and medium-frequency AC to grid-frequency AC conversion—plays a vital role in ensuring the performance of the SST. The modulation techniques used, the frequency characteristics of each stage, and the final transformation function have been elaborated to provide a clearer understanding of the system's operation. This comprehensive explanation highlights both the complexity and the potential for optimization in baseline SST designs, underscoring the need for more efficient and simplified configurations.

III. STRUCTURE AND OPERATION OF THE PROPOSED AM MODULATION

The structure of the proposed SST in this paper, as shown in Fig. 4, is significantly different from that of the conventional SST design discussed earlier. Unlike the conventional SST, which typically consists of multiple stages, the proposed converter operates with only two stages: a multilevel CHB inverter in the first stage and an AC-AC converter at the secondary side of the transformer in the second stage. This streamlined configuration is the key innovation of this paper, and it leads to several advantages, such as reduced complexity, lower cost, and enhanced overall efficiency compared to baseline SST designs.

The key idea behind this new configuration is the integration of the multilevel inverter with the AC-AC converter on the primary side of the medium-frequency transformer. In this design, the transformer's operating frequency (denoted as f_2) is used directly to convert the DC input voltage into a medium-frequency waveform with grid frequency envelope. This medium-frequency waveform is then transmitted through the transformer, where its amplitude is adjusted by the transformer turns ratio to reach the required voltage level. On the secondary side of the transformer, the AC-AC converter extracts a pure sinusoidal waveform with the grid frequency f_1, which can then be injected into the grid.

This approach significantly simplifies the conversion process while maintaining the essential functionalities of a baseline SST, such as voltage conversion, frequency decoupling, and active/reactive power control. Below, we will discuss the operating principles of the proposed SST stages in more detail.

A. STAGE ONE:

The first stage of the proposed SST involves a multilevel inverter, which is responsible for converting the input DC voltage into a medium-frequency AC voltage. The hardware structure of this stage is similar to that of the first stage in the baseline SST design. However, the key difference lies in the modulation type used for generating the reference waveform for the inverter. In the baseline design, the first stage of SST uses a standard modulation technique, but in this proposed design, we combine the transformation functions of both the first and second stages of the baseline SST. The transformation function in this case is expressed as:

$$F_1(t) = Asin(\omega_1 t) \times (-1)^{[\omega_2 t]} \quad (5)$$

A is the modulation index, ω_1 is the grid frequency, and ω_2 is the transformer's operating frequency. This modulation technique effectively combines the sinusoidal waveform of the grid frequency ω_1 with a modulating function that is determined by the transformer's operating frequency ω_2. The resulting reference waveform is illustrated in Fig. 5. By using this reference waveform, the switching of the multilevel inverter is facilitated in a manner that alters the output polarity at the operating frequency ω_2, generating a waveform that closely follows the desired output.

To generate this output, the proposed SST uses a combination of sinusoidal pulse width modulation (SPWM) and the aforementioned modulation scheme. The SPWM technique allows the inverter to produce a high-quality output voltage with low harmonic distortion, while the combined modulation method ensures that the output waveform has the desired characteristics. The switching signals and output voltages of the proposed five-level inverter are shown in Figs. 6-10. These figures demonstrate the control signals used to drive the inverter switches, as well as the resultant output voltage waveforms.

The use of the multilevel inverter at this stage is critical for achieving high power quality and efficient voltage conversion. The five-level inverter ensures that the voltage steps smoothly from one level to the next, reducing the Total Harmonic Distortion (THD) in the output waveform and making it more suitable for grid connection. The reduced THD is especially beneficial in applications like renewable energy integration, where maintaining a clean and stable output waveform is essential for synchronization with the grid.

B. STAGE TWO:

The second stage of the proposed SST involves an AC-AC converter located on the secondary side of the transformer. This converter takes the medium-frequency waveform generated by the primary-side multilevel inverter and transforms it into a pure sinusoidal waveform that matches the grid frequency (f_1). This step is critical for ensuring that the output power can be injected into the grid in a synchronized manner, without causing any issues related to frequency mismatches or harmonic distortion.

The AC-AC converter on the secondary side operates using a zero-crossing circuit, which detects the points at which the voltage waveform crosses zero and adjusts the converter's switching accordingly. By doing so, the converter ensures that the output waveform is perfectly synchronized with the grid frequency. This synchronization allows for smooth power injection into the grid, minimizing the possibility of harmonic distortion and maintaining the stability of the overall power system.

The reference voltage for the AC-AC converter is shown in Fig. 11, and it is used to control the output voltage of the transformer. The output voltage is adjusted in such a way that it aligns precisely with the grid frequency, as illustrated in Fig. 12. This ensures that the waveform injected into the grid is a clean sinusoidal waveform, which is essential for grid compliance and efficient power delivery.

The function of the AC-AC converter at this stage is given by the following equation:

$$F_2(t) = (-1)^{[\omega_2 t]} \quad (6)$$

This function represents the modulation applied to the medium-frequency waveform to produce a grid-synchronized output voltage. The converter's primary role is to remove any medium-frequency components from the waveform and ensure that only the grid frequency remains in the final output.

The overall function of the proposed SST can be described as the product of the functions from the multilevel inverter, the transformer, and the secondary side AC-AC converter. The general formula for this converter is expressed as:

$$F(t) = N \times F_1(t) \times F_2(t) = NAsin(\omega_1 t) \quad (7)$$

This formula illustrates how the system's output is determined by the modulation and transformation functions of the two stages. As in the baseline SST design, the output frequency and voltage are controlled by the multilevel inverter at the primary side. However, in the proposed design, the removal of the primary side AC-AC converter (which exists in the baseline three-stage SST) results in a simpler, more efficient system.

The elimination of the primary AC-AC converter is a key feature of the proposed SST design. This reduction in the number of converters not only simplifies the overall hardware structure but also reduces the number of semiconductor switches required to operate the converter. In baseline SSTs, the primary AC-AC converter typically requires a large number of semiconductor switches to control the flow of power (due to lower voltage and higher current level), leading to higher losses and increased complexity. By removing this stage, the proposed design eliminates at least 4 bidirectional or 8 semiconductor switches, leading to reduced losses and improved efficiency.

Furthermore, the elimination of the primary AC-AC converter contributes to a significant reduction in the volume and dimensions of the SST. With fewer components, the overall size of the converter is reduced, making it more compact and suitable for applications where space is limited. This reduction in size also leads to a decrease in overall system costs, as fewer components are required for manufacturing and maintenance.

The proposed SST design represents a significant improvement over baseline designs, offering a simplified, more efficient, and cost-effective solution for high-voltage, high-power applications. By reducing the number of energy conversion stages and eliminating the primary AC-AC converter, the proposed design offers several advantages, including lower semiconductor count, reduced losses, and smaller physical dimensions. These improvements make the proposed SST particularly attractive for integration into renewable energy systems, electric grids, and other power distribution applications where efficiency, size, and cost are critical factors. The use of a multilevel inverter in combination with a secondary AC-AC converter ensures that the system operates at high efficiency while maintaining the required power quality for grid synchronization.

In this study, a comparative analysis is conducted between the proposed, baseline and conventional SSTs [4]. The proposed SST utilizes only one switching stage (beside the solar inverter with multilevel structure), whereas conventional SSTs rely on three distinct stages (AC-DC, DC-DC, and DC-AC) and the baseline one two conversion stages (two AC-AC converters). This reduction in conversion stages not only simplifies the control strategy but also leads to improved efficiency and reduced component count. The results of this comparison are reported in Table II. It should be noted that for the sake of fair comparison, all the SSTs are considered for PV application and a five-level solar inverter is concluded in the comparison.

Regarding semiconductor switch count, the proposed SST requires only 12 switches (considering the inverter switches), while the baseline and conventional SSTs require at least 16 and 20, respectively due to additional conversion stages. This reduction in switches minimizes conduction and switching losses, leading to an overall increase in power efficiency. Specifically, the total switching losses in the proposed SST are approximately 150 W, whereas in the baseline and conventional SST, they exceed 200 W and 250 W, respectively due to the additional conversion stages.

Efficiency is another critical aspect where the proposed SST outperforms its conventional counterpart. The efficiency of the proposed SST is measured at 94%, whereas the conventional SST achieves below 90%. This improvement results from the elimination of intermediate DC-DC conversion and the implementation of a more streamlined energy transfer process.

Furthermore, the system cost is significantly lower in the proposed SST due to fewer components and a simpler circuit topology. Baseline and conventional SSTs require additional converters, passive elements, and complex control systems, increasing both manufacturing costs and maintenance expenses. In contrast, the proposed SST achieves cost savings by minimizing the number of active power devices and simplifying thermal management requirements.

Another key factor in favor of the proposed SST is its higher reliability. Due to fewer components and reduced stress on switches, the proposed SST exhibits enhanced reliability and longer operational lifespan compared to the other two SSTs, which contain more components, experience higher thermal stress, and require more advanced cooling mechanisms.

These improvements highlight the practical advantages of the proposed SST, making it a more viable solution for PV application where high efficiency, reduced cost, minimal component count, and higher reliability are crucial.

IV. SIMULATION

This section presents the detailed simulation results for the proposed Solid-State Transformer (SST) configuration, which is equipped with a five-level inverter. The key parameters used in the simulation are summarized in Table I. In this simulation setup, the five-level inverter comprises two cells, each powered by independent voltage sources with a value of V_{dc}. These independent voltage sources allow for the flexibility needed to implement multi-level modulation techniques, enhancing the performance of the inverter by reducing harmonic distortion in the output voltage.

The switching frequency of the inverter is set at 25 kHz, while the modulation frequency is fixed at 2.5 kHz. The grid frequency, as expected for typical grid-tied systems, is set at 50 Hz. The use of a Phase-Locked Loop (PLL) circuit in the primary inverter is crucial for synchronizing the output waveform to the grid frequency. The PLL circuit locks the frequency of the inverter to the grid voltage, ensuring that the inverter operates in perfect harmony with the power grid. The feedback from the grid voltage is employed to continuously adjust and synchronize the inverter output, guaranteeing minimal phase difference and high-quality power delivery.

The inverter output voltage for the first stage is shown in Fig. 13 with the amplitude of 200 V. This voltage waveform is characterized by a 50 Hz envelope, representing the grid frequency, with a 2.5 kHz main harmonic. The primary function of this stage is to shape the voltage into a form suitable for grid injection, with minimal harmonic distortion. The output current generated by the MLI reaches a maximum of 25 A, which is in line with the expected current levels for the designed system.

Following the generation of the 2.5 kHz medium-frequency waveform, the secondary AC-AC converter is employed to eliminate the medium-frequency component and extract the 50 Hz grid frequency. As shown in Fig. 14 and Fig. 15, the output voltage and current now exhibit the primary harmonic at 50 Hz, with the high-frequency noise effectively filtered out. This ensures that the waveform injected into the grid matches the characteristics of the utility grid, maintaining the quality of power transmission.

It should be noted that the proposed SST has a impedance-based load in the simulation to be as similar as possible to the test setup. Further, the voltage across the inductor, representing the difference between the resistor voltage and the output voltage of the AC-AC converter, is displayed in Fig. 16. This voltage waveform is crucial for understanding the dynamic behavior of the converter and how the energy is transferred from the primary to the secondary side of the transformer.

The simulation results reveal that the output voltage THD is 26.95%, while the THD for the output current is much lower, at 1.71%. These results indicate that while the voltage waveform contains some harmonic distortion, it remains within acceptable limits for grid-tied applications. For connecting the proposed SST to the network a suitable low-pass filter should be designed and placed in the output of the proposed SST. In conclusion, the simulation results demonstrate that the proposed SST configuration, equipped with a five-level inverter and a secondary AC-AC converter, work as it was expected.

V. EXPERIMENTAL EVALUATION

This section presents the experimental validation of the proposed SST by utilizing an operational prototype, which serves to confirm the accuracy of the simulation results. The test setup for the prototype, shown in Fig. 17, consists of several key components, including an AC-AC converter and a five-level inverter. The prototype features twelve isolated 15 V voltage sources based on flyback-converter. These voltage sources are incorporated into the circuit to power twelve gate driver circuits, which are responsible for controlling the switching operations of the various power devices within the SST. In addition, two DC-DC converters are used to simulate the DC voltage sources. These converters represent the photovoltaic (PV) plants, supplying the necessary DC voltage to the system in a manner that mimics the output of a solar power generation setup.

For implementing the control system an ARM/STM32F303 microcontroller board is employed. This microcontroller plays a critical role in implementing the control algorithms, ensuring that the SST operates as intended. Specifically, the ARM-based control system manages the switching operations of the two cells of CHB inverter.

Fig. 18, Fig. 19, and Fig. 20 show the resulting medium-frequency voltage produced by the CHB inverter. The maximum amplitude of the inverter voltage reaches 200 V, with a peak-to-peak amplitude of approximately 400 V. This

voltage waveform is crucial for the operation of the SST, as it represents the primary output from the inverter that will be transformed by the medium-frequency transformer. To ensure accurate control, a voltage sensor is employed to measure the medium-frequency voltage, which allows for the precise determination of the zero-crossing time. This zero-crossing detection is essential for generating the control signal of the AC-AC converter, ensuring that the output waveform is synchronized and accurate.

When the SST is connected to the load (described in Table I), the resulting output voltage and current waveforms are measured and recorded. The voltage waveform, current waveform, and the inductor voltage are displayed in Fig. 21 to Fig. 23, providing a comprehensive view of the system's performance under operational conditions. The experimental results validate the theoretical and simulated performance of the proposed SST, confirming that the system is capable of generating stable and reliable output voltages and currents with minimal distortion.

Through this experimental validation, it is evident that the proposed SST operates effectively, with the control system functioning as expected. The elimination of medium-frequency harmonics and the generation of a clean 50 Hz output voltage demonstrate the feasibility of the SST for practical applications, such as integration with renewable energy sources like photovoltaic plants. The experimental results not only support the accuracy of the simulation but also highlight the potential of the proposed SST design in real-world scenarios.

VI. CONCLUSION

In this paper, a new modulation method, referred to as AM modulation, is introduced for the multilevel inverter in solid-state transformer converter. The proposed modulation technique aims to enhance the performance of SSTs by simplifying the overall converter structure while maintaining high efficiency and reliability. The analytical analysis of the AM modulation method was conducted, and the results were carefully evaluated using MATLAB simulations. These simulations validated the theoretical framework, showing promising outcomes in terms of voltage and current waveforms, as well as harmonic distortion.

In addition, an experimental prototype of the proposed SST was designed and tested to further validate both the analytical and simulation results. The prototype testing provided experimental measurements that confirmed the viability of the proposed system. The results demonstrated that the new modulation technique significantly reduces the number of energy conversion stages and power electronic devices required in comparison to the baseline SST designs. This reduction leads to a substantial decrease in power losses, which directly enhances the overall system efficiency.

Furthermore, the proposed SST with AM modulation results in a reduction in the volume and physical dimensions of the system. This not only makes it more suitable for applications with space and weight constraints but also contributes to a decrease in the overall cost of the system. Therefore, the proposed modulation method is an attractive solution for improving the performance, efficiency, and cost-effectiveness of future SST-based applications. Future research can focus on enabling full grid-connected operation of the proposed SST. This includes investigating synchronization algorithms, compliance with grid codes, and implementing appropriate protection schemes. Additionally, hardware-in-the-loop (HIL) testing and real-time simulations can be conducted to evaluate the system’s performance under grid-connected conditions.

REFERENCES

[1] Huber, J. and Kolar, J. "Volume/weight/cost comparison of a 1MVA 10 kV/400 V solid-state against a conventional low-frequency distribution transformer", *2014 IEEE Energy Conversion Congress and Exposition (ECCE)*, Pittsburgh, USA (2014). DOI: 10.1109/ECCE.2014.6954023

[2] Feng, J., Chu, W., Zhang, Z., et al. "Power Electronic Transformer Based Railway Traction Systems: Challenges and Opportunities", *IEEE Journal of Emerging and Selected Topics in Power Electronics*, 5(3), pp. 1237-1253 (2017). DOI: 10.1109/JESTPE.2017.2685464

[3] Verma, N., Singh, N., and Yadav, S. "Solid State Transformer for Electrical System: Challenges and Solution", *2nd International Conference on Electronics, Materials Engineering & Nano-Technology (IEMENTech)*, Kolkata, India (2018). DOI: 10.1109/IEMENTECH.2018.8465315

[4] Huber, J. and Kolar, J. "Solid-State Transformers: On the Origins and Evolution of Key Concepts", *IEEE Industrial Electronics Magazine*, 10(3), pp. 19-28 (2016). DOI: 10.1109/MIE.2016.2588878

[5] Han, B., Choi, N., and Lee, J. "New Bidirectional Intelligent Semiconductor Transformer for Smart Grid Application", *IEEE Transactions on Power Electronics*, 29(8), pp. 4058-4066 (2013). DOI: 10.1109/TPEL.2013.2284009

[6] Falcones, S., Mao, X., and Ayyanar, R. "Topology Comparison for Solid State Transformer Implementation", *IEEE PES General Meeting*, Minneapolis, USA (2010). DOI: 10.1109/PES.2010.5590086

[7] Liu, B., Zha, Y., Zhang, T., et al. "Solid state transformer application to grid connected photovoltaic inverters", *2016 International Conference on Smart Grid and Clean Energy Technologies (ICSGCE)*, Chengdu, China (2017). DOI: 10.1109/ICSGCE.2016.7876063
[8] Foureaux, N., Filho, B., and Brito, J. "Cascaded multilevel SST medium voltage converter for solar applications", *2015 9th International Conference on Power Electronics and ECCE Asia (ICPE-ECCE Asia)*, Seoul, Korea (2015). DOI: 10.1109/ICPE.2015.7167874
[9] Vijay Autkar, K. and Dhamse, S. "Solid State Transformer for Doubly Fed Induction Generator Based Wind Energy Conversion System: A Review", *International Conference on Computation of Power, Energy, Information and Communication (ICCPEIC)*, Chennai, India (2018). DOI: 10.1109/ICCPEIC.2018.8525189
[10] Syed, I. and Khadkikar, V. "Replacing the Grid Interface Transformer in Wind Energy Conversion System with Solid-State Transformer", *IEEE Transactions on Power System*, 32(3), pp. 2152–2160 (2017). DOI: 10.1109/TPWRS.2016.2614692
[11] Paladhi, S. and Ashok, S. "Solid State Transformer Application in Wind Based DG System", *IEEE International Conference on Signal Processing, Informatics, Communication and Energy Systems (SPICES)*, Kozhikode, India (2015). DOI: 10.1109/SPICES.2015.7091563
[12] Heydt, G. "Future renewable electrical energy delivery and management systems: Energy reliability assessment of FREEDM systems", *IEEE PES Gen. Meet. PES 2010*, Minneapolis, USA (2010). DOI: 10.1109/PES.2010.5589348
[13] Rodríguez, J., Lai, J., and Peng F. "Multilevel Inverters: A Survey of Topologies, Controls, and Applications", *IEEE Transactions on Industrial Electronics*, 49(4), pp. 724–738 (2002). DOI: 10.1109/TIE.2002.801052
[14] Abdoli, H., Khorsandi, A., Eskandari, B., et al. "A New Reduced Switch Multilevel Inverter for PV Applications", *11th Power Electronics, Drive Systems, and Technologies Conference (PEDSTC)*, Tehran, Iran, (2020). DOI: 10.1109/PEDSTC49159.2020.9088508
[15] Babaki, A., Vaez-Zadeh, S., Zakerian, A., et al. "Analysis and Control of Wireless Motor Drives with a Single Inverter in Primary Side", *IEEE Transactions on Energy Conversion*, 36(2), pp. 930–939 (2021). DOI: 10.1109/TEC.2020.3026072
[16] Natanzi, A., Vaez-Zadeh, S., Babaki, A., et al. "A Single-Phase Wireless Power Transfer System with a High-Frequency AC Link Converter in the Secondary for Three-Phase Applications", *12th Power Electronics, Drive Systems, and Technologies Conference (PEDSTC)*, Tabriz, Iran, (2021). DOI: 10.1109/PEDSTC52094.2021.9405892
[17] Molla-ahmadian, H., Shafiee, M., Khorasani, J., et al. "Integrated Modeling of Bidirectional Solid-State Transformers with an Arbitrary Number of H-Bridge Converters", *Scientia Iranica*, Early access (2024). DOI: 10.2139/ssrn.4173699
[18] Ding, C., Zhang, H., Chen, Y., et al. "Research on Control Strategy of Solid State Transformer Based on Improved MPC Method", *IEEE Access*, 11(1), pp. 9431–9440 (2023). DOI: 10.1109/ACCESS.2023.3240310
[19] Agarwal, R., Li, H., Guo, Z., et al. "The Effects of PWM with High dv/dt on Partial Discharge and Lifetime of Medium-Frequency Transformer for Medium-Voltage (MV) Solid State Transformer Applications", *IEEE Transactions on Industrial Electronics*, 70(4), pp. 3857-3866 (2023). DOI: 10.1109/TIE.2022.3174243
[20] Zheng, L., Kandula, R., Kandasamy, K., et al. "New modulation and impact of transformer leakage inductance on current-source solid-state transformer", *IEEE Transactions on Power Electronics*, 37(1), pp. 562-576 (2022). DOI: 10.1109/TPEL.2021.3101811
[21] Zheng, L., Marellapudi, A., Chowdhury, V., et al. "Solid-state transformer and hybrid transformer with integrated energy storage in active distribution grids: Technical and economic comparison, dispatch, and control", *IEEE Journal of Emerging and Selected Topics in Power Electronics*, 10(4), pp. 3771-3787 (2022). DOI: 10.1109/JESTPE.2022.3144361
[22] Zheng, L., Han, X., Kandula, R., et al. "DC-link current minimization control for current source converter-based solid-state transformer", *IEEE Transactions on Power Electronics*, 37(10), pp. 11865-11875 (2022). DOI: 10.1109/TPEL.2022.3178433
[23] El Shafei, A., Ozdemir, S., Altin, N., et al. "A high power high frequency transformer design for solid-state transformer applications", *8th International Conference on Renewable Energy Research and Applications (ICRERA)*, Brasov, Romania (2019). DOI: 10.1109/ICRERA47325.2019.8996515
[24] Zheng, L., Kandula, R., and Divan, V. "Multiport Control With Partial Power Processing in Solid-State Transformer for PV, Storage, and Fast-Charging Electric Vehicle Integration", *IEEE Transactions on Power Electronics*, 38(2), pp. 2606-2616 (2023). DOI: 10.1109/TPEL.2022.3211000
[25] Li, Z., Qin, Z., and Mirzadarani, R. "Comparison of modular multilevel converter-based solid-state transformer for AC-DC application", *8th IECON 2023- 49th Annual Conference of the IEEE Industrial Electronics Society*, Singapore, Singapore (2023). DOI: 10.1109/IECON51785.2023.10312314
[26] Rehman, A., Daud, M., Haider, S., et al. "Comprehensive review of solid-state transformers in the distribution system: From high voltage power components to the field application", *Symmetry*, 14(10), pp. 1-23 (2022). DOI: 10.3390/sym14102027
[27] Rehman, A. and Ashraf, M. "Design and analysis of PWM inverter for 100KVA solid-state transformer in a distribution system", *IEEE Access*, 7(1), pp. 140152-140168 (2019). DOI: 10.1109/ACCESS.2019.2942422
[28] Deswal, D. and Leon, F. "Distributed dual model for high-frequency transformer windings electromagnetic transients and solid-state transformers", *IEEE Open Access Journal of Power and Energy*, 9(1), pp. 549-559 (2022). DOI: 10.1109/OAJPE.2022.3208251

[29] Cervone, A., Li, Z., and Dujic, D. "Modularized diode rectifiers: A new family of solid-state transformers", *IEEE Transactions on Power Electronics*, 40(4), pp. 4747-4751 (2025). DOI: 10.1109/TPEL.2024.3520237
[30] Da Silva Jr, R., Borges, V., Possamai, C., et al. "Solid-state transformer for power distribution grid based on a hybrid switched-capacitor LLC-SRC converter: Analysis, design, and experimentation", *IEEE Access*, 8(1), pp. 141182-141207 (2020). DOI: 10.1109/ACCESS.2020.3013188
[31] Li, Y., Zhang, Y., Cao, R., et al. "Redundancy design of modular DC solid-state transformer based on reliability and efficiency evaluation", *CPSS Transactions on Power Electronics and Applications*, 6(2), pp. 115-126 (2021). DOI: 10.24295/CPSSTPEA.2021.00010
[32] Shafei, A., Ozdemir, S., and Altin, A. "Development of a medium voltage high power high frequency four-port solid-state transformer", *CES Transactions on Electrical Machines and Systems*, 6(1), pp. 95-104 (2022). DOI: 10.30941/CESTEMS.2022.00013
[33] Li, Z., Mirzadarani, R., Niasar, M., et al. "Medium-voltage solid-state transformer design for large-scale H2 electrolyzers", *IEEE Open Journal of Power Electronics*, 5(1), pp. 936-955 (2024). DOI: 10.1109/OJPEL.2024.3414151
[34] Hannan, M., Ker, P., Lipu, S., et al. "State of the art of solid-state transformers: Advanced topologies, implementation issues, recent progress and improvements", *IEEE Access*, 8(1), pp. 19113-19132 (2020). DOI: 10.1109/ACCESS.2020.2967345

List of Figures:

FIGURE 22. Output current of AC-AC converter in prototype.

FIGURE 23. Voltage across load inductor in prototype.

List of Tables:

Table I: SYSTEM PARAMETERS

Table II: SSTS TOPOLOGY COMPARISON

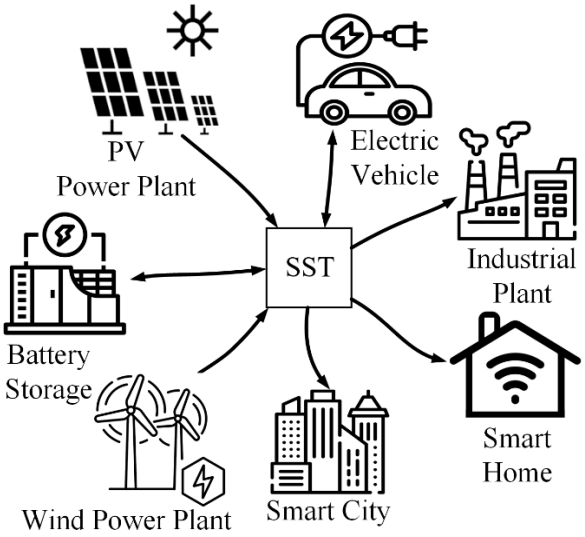

Fig 1. Applications of solid-state transformer.

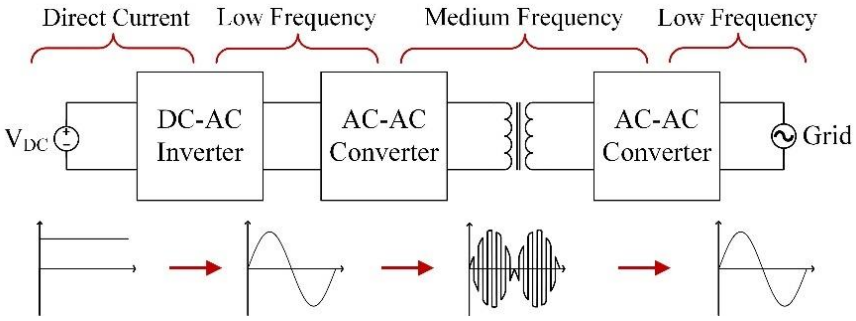

Fig 2. Baseline SST with two AC-AC converters.

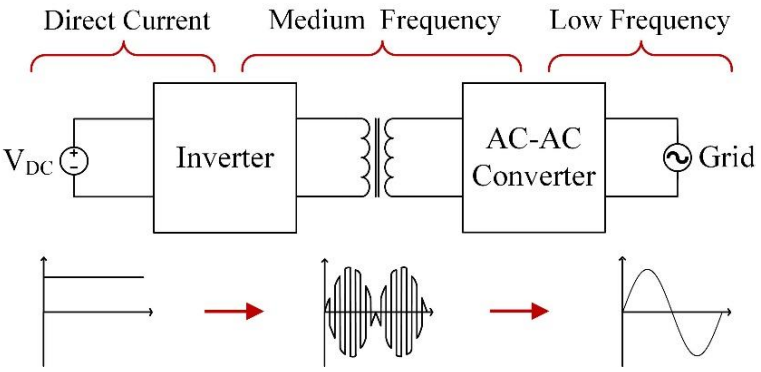

Fig 3. Proposed SST Structure.

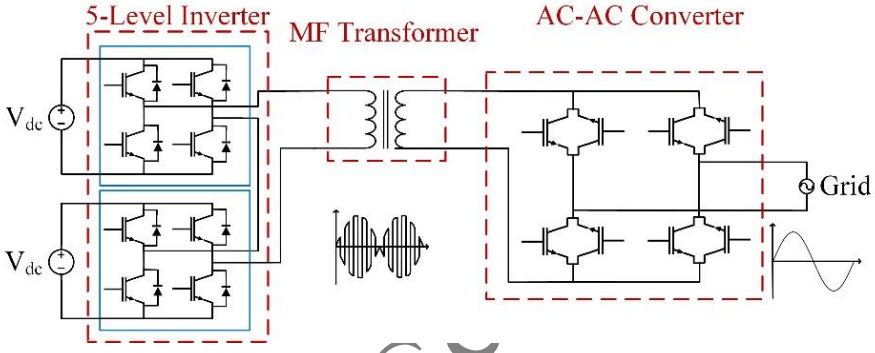

Fig 4. Proposed SST with an innovative modulation technique for the five-level inverter.

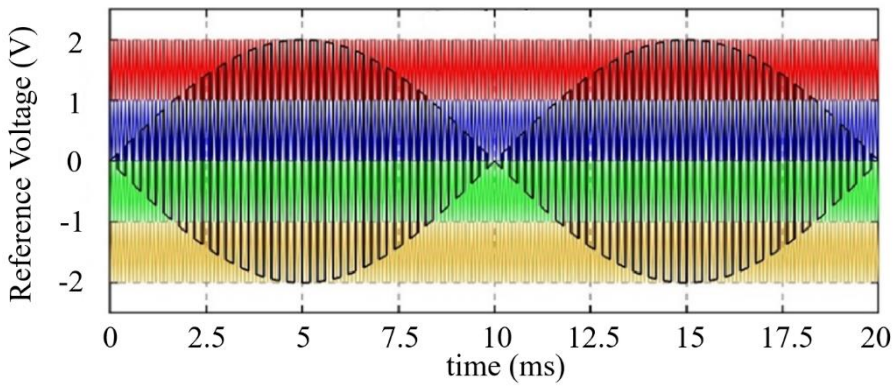

Fig 5. Reference voltage of the proposed five-level inverter.

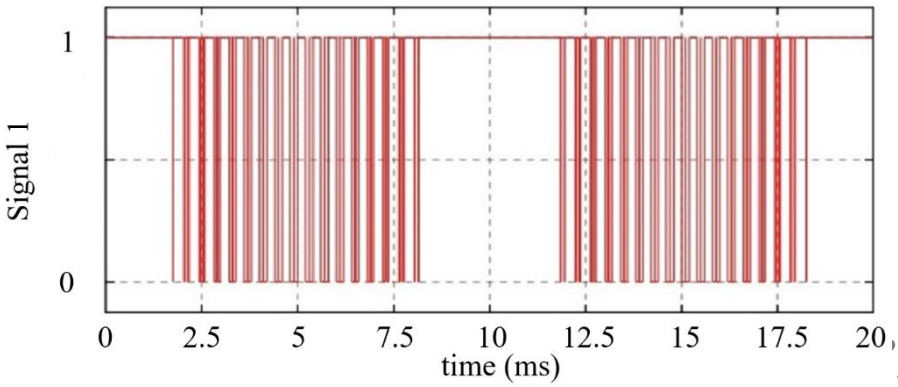

Fig 6. Switching signal for cell 1 of proposed five-level inverter.

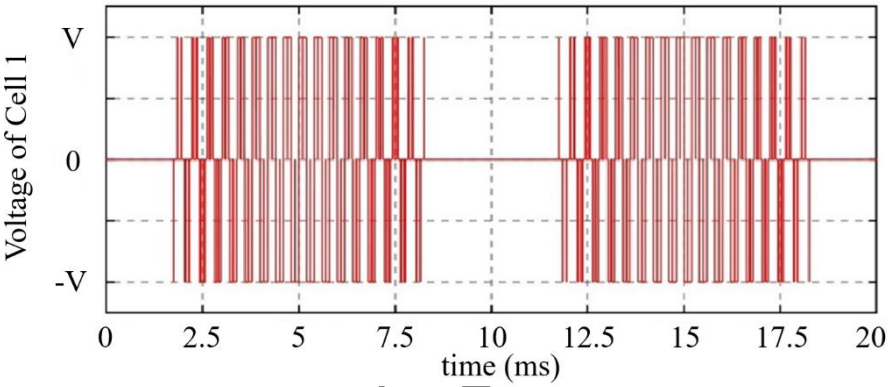

Fig 7. Cell 1 output voltage of proposed five-level inverter.

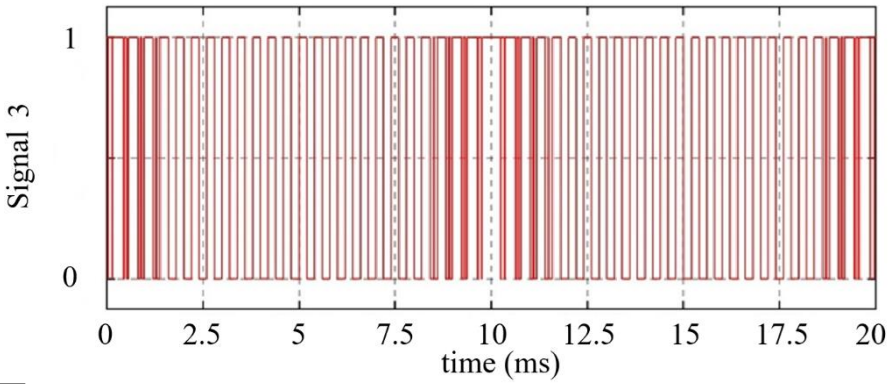

Fig 8. Switching signal for cell 2 of proposed five-level inverter.

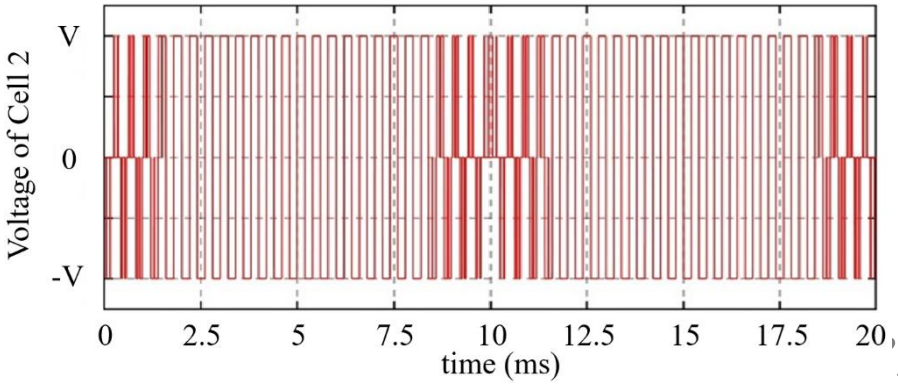

Fig 9. Cell 2 output voltage of the proposed five-level inverter.

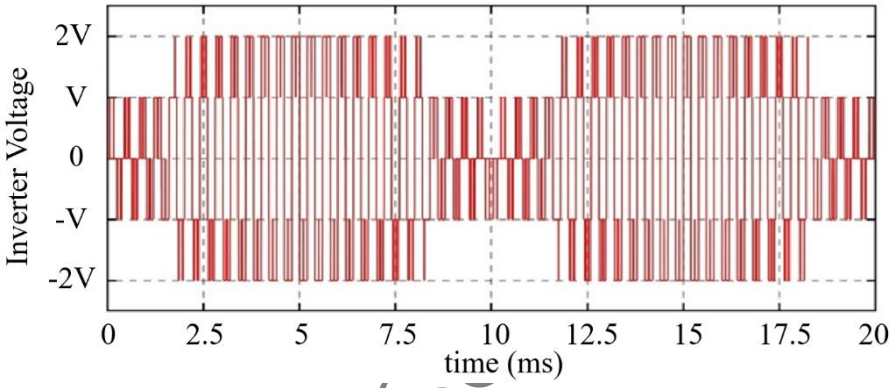

Fig 10. Output voltage of the proposed five-level inverter.

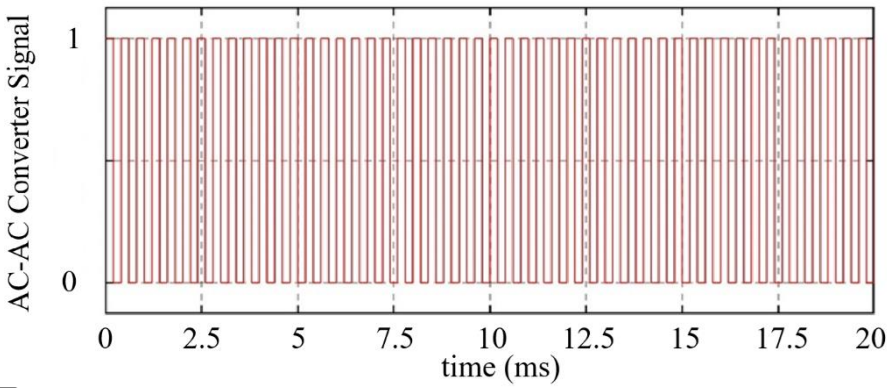

Fig 11. AC-AC converter's reference voltage.

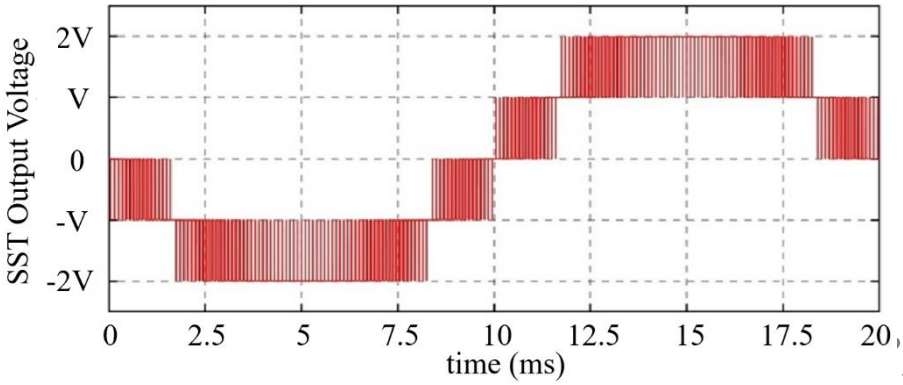

Fig 12. AC-AC converter's output voltage.

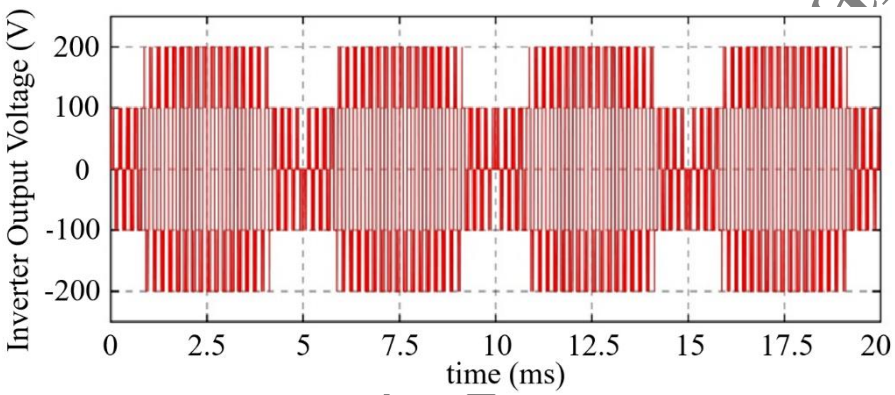

Fig 13. Five-level inverter output voltage.

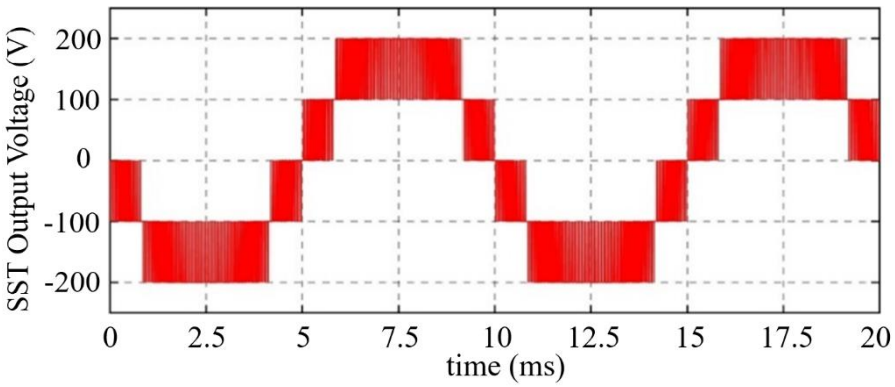

Fig 14. Output voltage of AC-AC converter.

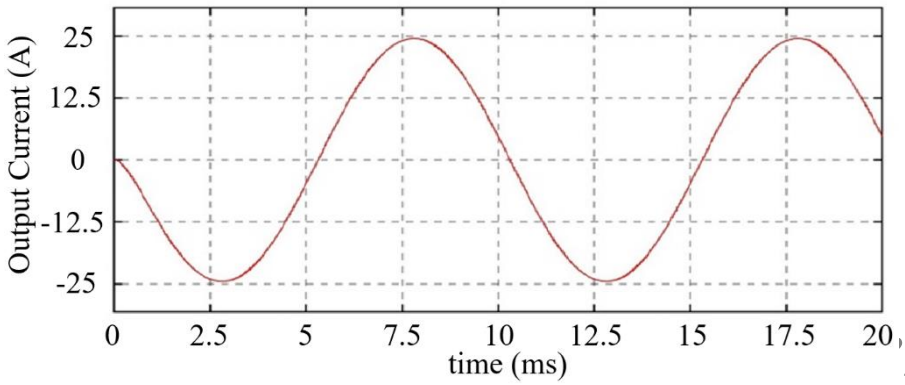

Fig 15. Output current of AC-AC converter.

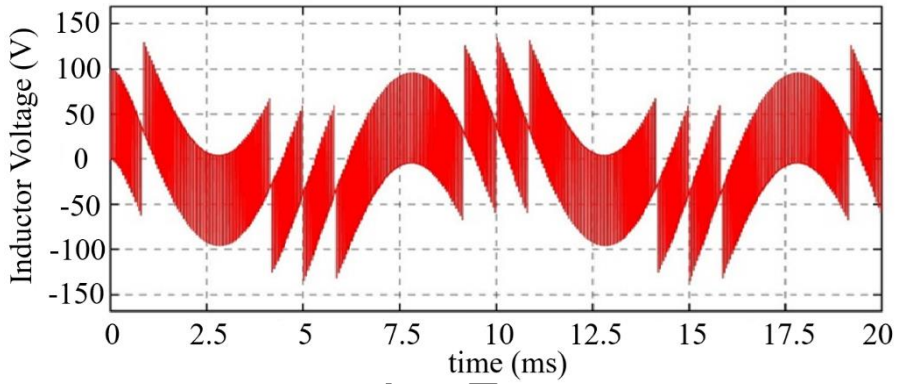

Fig 16. Voltage across the load inductor.

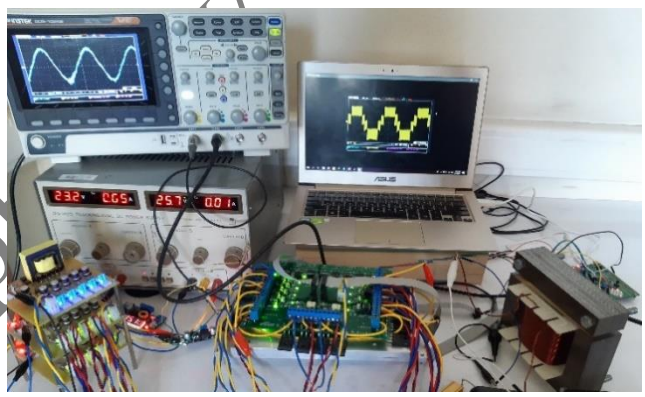
Fig 17. Prototype test setup.

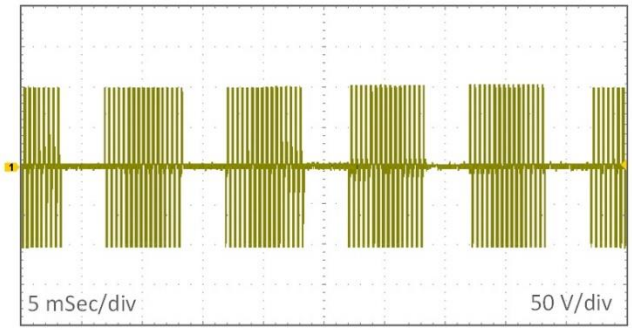

Fig 18. Output voltage for Cell 1 of the primary five-level inverter.

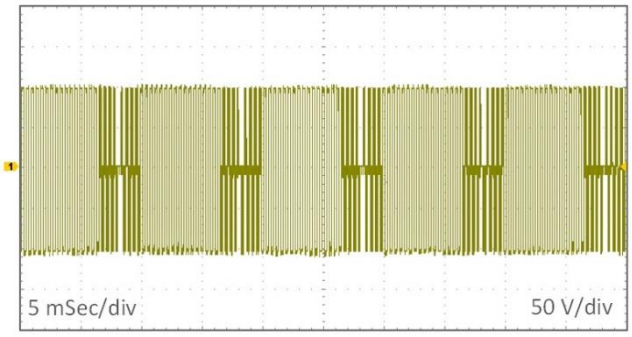

Fig 19. Output voltage for Cell 2 of the primary five-level inverter.

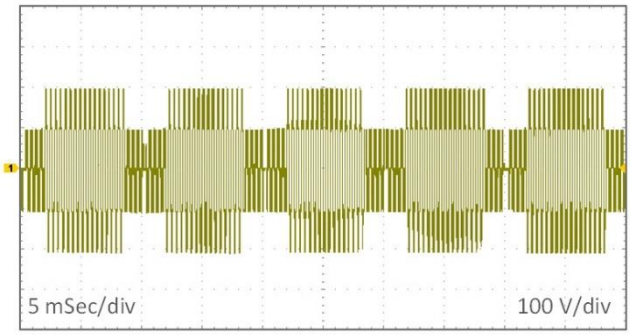

Fig 20. Output voltage of Five-level inverter in prototype.

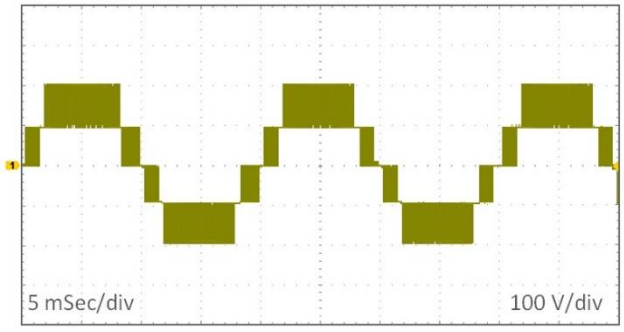

Fig 21. Output voltage of AC-AC converter in prototype.

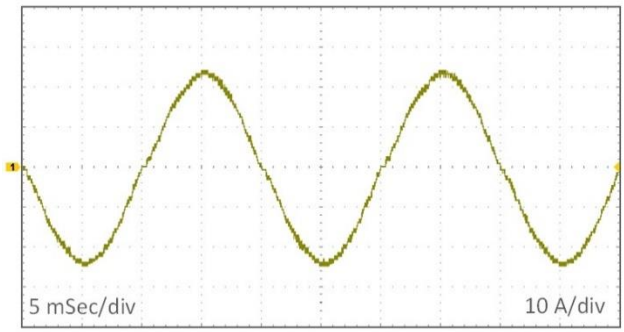

Fig 22. Output current of AC-AC converter in prototype.

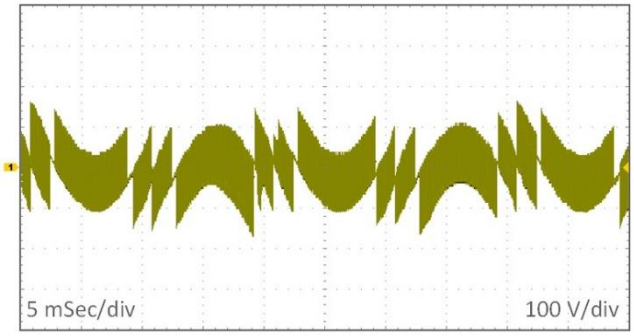

Fig 23. Voltage across load inductor in prototype.

TABLE I
SYSTEM PARAMETERS

Symbol	Quantity	Value
RL	Load resistance	8 Ω
LL	Load inductance	5 mH
Vdc	DC voltage sources	100 (Volts)
fsw	Switching frequency	25000 (Hz)
fm	Modulation frequency	2500 (Hz)
fgrid	Grid frequency	50 (Hz)
N	Number of cells	2
n	Transformer Turn Ratio	1
-	IGBT Part Number	IKW25N120T2
-	Driver Part Number	HCPL-316J
-	Microcontroller Part Number	STM32F303VCT6
P	Power Rating	2500 (Watts)

TABLE II
SSTs TOPOLOGY COMPARISON

Criterion	Proposed SST	Baseline SST	Conventional SST
Number of Conversion Stages	2 stages (AM-Modulated Multilevel Inverter + AC-AC)	3 stages (Multilevel Inverter, AC-AC, AC-AC)	4 stages (Multilevel Inverter + AC-DC, DC-DC, DC-AC)
Semiconductor Switch Count	12 switches	16 switches	+20 switches
Total Switching Losses (W)	150 W	~ 200 W	~ 250 W
Power Efficiency (%)	94	~92	~90
System Cost	Low (Fewer parts and simplified design)	High (More parts and complex design)	Very High (Even more parts and very complex design)
Reliability	High (Fewer parts and reduced stress on switches)	Low (More parts and higher temperature-related stress)	Very Low (Even more parts and much higher thermal stress)

Biographies:

HESAMODIN ABDOLI was born in Malayer, Iran, in 1996. He received the B.S. degree in Electrical Engineering from Shiraz University of Technology, Shiraz, Iran, in 2018, and the M.Sc. degree in Electrical Engineering from Amirkabir University of Technology, Tehran, Iran, in 2021. His research interests primarily focus on power electronics, specifically converters such as multilevel inverters (MLIs), and electrical drive systems.

GHASEM REZAZADEH was born in Freydoonkenar, Iran, in 1990. He received: 1) the B.S. degree in electrical engineering from Shahid Beheshti University, in 2012; 2) the M.Sc. degree from Sharif University of Technology, Tehran, Iran, in 2014; and 3) the Ph.D. degree in a co-supervision in between Sharif University of Technology and University of Picardie Jules Verne, Amiens, France, in 2021. He has been with the School of Electrical and Computer Engineering, College of Engineering, University of Tehran since 2023 where he is currently an Assistant Professor. His research interests include design, modeling, and control of electrical machines and power electronics converters.

JAVAD SHOKROLLAHI MOGHANI was born in Tabriz, Iran, in 1956. He received the B.Sc. degree from South Bank Polytechnic, London, U.K., in 1982, the M.Sc. degree from the Loughborough University of Technology, Loughborough, U.K., in 1984, and the Ph.D. degree from the University of Bath, Bath, U.K., in 1995, all in electrical engineering.

From 1984 to 1991, he was with the Department of Electrical Engineering, Amirkabir University of Technology, Tehran, Iran, where he is currently an Associated Professor. His research interests include electromagnetic modeling and design using the finite-element method, power electronics, and electric drives.

SADEGH VAEZ-ZADEH (Senior Member, IEEE) received the B.Sc. degree from the Iran University of Science and Technology, Tehran, Iran, in 1985, and the M.Sc. and Ph.D. degrees from Queen's University, Kingston, ON, Canada, in 1993 and 1997, respectively, all in electrical engineering. He had been with several research and educational institutions in different positions before joining the University of Tehran as an Assistant Professor, in 1997, where he became an Associate Professor, in 2001, and a Full Professor, in 2005.

He served the university as the Head of the Power Division, from 1998 to 2000, and is currently the Director of the Advanced Motion Systems Research Laboratory, which he founded in 1998. He has also been the Director of the Electrical Engineering Laboratory, since 1998. He has coauthored over 200 research articles in these areas and holds a U.S. patent. He is the author of Control of Permanent Magnet Synchronous Motors (Oxford University Press, 2018). His research interests include advanced rotary and linear electric machines and drives, wireless power transfer, renewable energy integration, and energy policy. He is a member of the IEEE PES Motor Sub-Committee and Energy Internet Coordinating Committee. He has received several domestic and international awards for his contributions to the fields. He has been active in IEEE-sponsored conferences as the general chair, a keynote speaker, and as a member of technical and steering committees. He is an Editor of the IEEE Transactions on Energy Conversion, an Editor of the IEEE Transactions on Sustainable Energy, and a Subject Editor of IET Renewable Power Generation.